arXiv:2609.00446v2 [cs.LG] 2 Nov 2026

CRAD: Class-wise Reliability-Aware Distillation for Decentralized Heterogeneous Federated Learning

Baraa Bilbeisi[1,*] Mengchen Fan[2,*] Baocheng Geng[2] Qing Tian[2,†]
[1]Dept. of Electrical & Computer Engineering [2]Dept. of Computer Science
University of Alabama at Birmingham, AL, USA

Abstract

Conventional federated learning (FL) relies on parameter averaging, which forces clients to be doubly homogeneous: it demands an identical architecture and degrades under non-IID data. Real-world deployments usually break both assumptions. We sidestep both by building a decentralized knowledge distillation framework in which each client evaluates its peers' model snapshots on its own local data and distills from the resulting soft predictions. Because knowledge is transferred through the shared class posterior, clients are free to run different architectures; and because every teacher is evaluated on the student's own device, raw data never leaves the client, with no central server or public dataset required. Within this setting, we identify and address an under-examined problem: how to combine the peer teacher predictions. Existing methods, like uniform averaging, ignore how knowledge reliability varies across teachers and classes. We propose Class-wise Reliability-Aware Distillation (CRAD), which, per class, first discards teachers that disagree with the peer consensus and then takes a weighted average of the rest, weighting each teacher by its per-class reliability (precision, or inverse variance). Since the variance of an accuracy from n samples scales as $1/n$, support enters automatically: among the teachers that survive filtering, a teacher is trusted for a class to the degree that it is both accurate and well-evidenced for it. On CIFAR-10, CIFAR-100, and PathMNIST, across heterogeneous architectures under severe non-IID skew, CRAD consistently outperforms competing methods in global accuracy. Our code is publicly available at https://github.com/bbilbeis/CRAD.

1. Introduction

Federated learning (FL) has enabled collaborative training of machine learning models across distributed clients while keeping raw data local [23, 24]. However, a fundamental limitation in practical deployments is the architectural homogeneity imposed by parameter averaging [7, 16, 25]. This assumption is rarely satisfied in real-world FL systems [16, 27, 35]. Consider a network of hospitals collaborating to train a diagnostic imaging model. Each operates under distinct hardware and data availability: a large urban hospital may run a full-scale network on a GPU server, while a rural clinic can only afford a compact model on a low-power device. Autonomous-driving fleets face the same problem: vehicles carry different onboard hardware and run in different environments. Because participants in either setting cannot share raw data, FL is the natural solution [1, 14]. Yet standard FL fails here. Averaging across different architectures is undefined, since the weight tensors differ in shape and semantics [7, 20]. Forcing a shared architecture is no remedy. No single architecture suits all institutions without over-provisioning weak devices or under-using capable ones [27, 35], and averaging models that have each specialized to their own skewed data can produce a model worse than any individual specialist [2, 13, 36].

Existing FL methods fall into two groups, neither fully suited to decentralized, architecturally heterogeneous learning. Parameter-space consensus methods [15, 19, 31] curb client drift under non-IID data but still combine weights within a shared model space, so they remain inapplicable across incompatible architectures [16, 25]. Knowledge-distillation methods [11, 18, 20] instead exchange architecture-agnostic soft predictions, escaping the homogeneity constraint, but typically reintroduce a shared public dataset or a central server [8, 25], the very privacy and centralization costs FL is meant to avoid [22, 26]. These observations motivate our approach: a fully decentralized, peer-to-peer knowledge distillation (KD) framework in which clients collaborate without parameter averaging. Each client shares model snapshots, instantiates peer snapshots as local teachers, evaluates them on its own data, and distills from their combined soft predictions, with no public transfer set or central coordinator. Decentralized, public-data-free distillation of this kind is attractive because

*These authors contributed equally.
†Corresponding author: qtian@uab.edu

it is natively compatible with heterogeneous architectures, and it lets each client learn the classes it sees rarely or not at all [16]. But making this setting work surfaces a problem the FL distillation literature has largely left implicit: once a client holds a pool of peer teacher predictions, how should those predictions be combined to guide the student?

The default answer, inherited from ensemble distillation [20], is a uniform average over all peers. This is a poor choice under heterogeneity, where teacher reliability is uneven and class-dependent. The central question of our work is therefore how a client should weight its peer teachers, per class, accounting for both how accurate and how well-supported each teacher is (a class accuracy from few samples being itself unreliable), without a server, public data, or expensive tuning.

We answer with Class-wise Reliability-Aware Distillation (CRAD). Alongside its model snapshot, each client shares a compact class-wise statistics vector summarizing, for every class, how many validation samples it holds and how often it classifies them correctly. On receiving these statistics from its peers, a client works class by class: it first discards the teachers that hold insufficient samples of the class or whose predictions deviate most from the per-class peer consensus, then combines the survivors by inverse-variance (precision) weighting, so that each teacher counts in proportion to both the decisiveness and the statistical support of its class-accuracy estimate. Because the variance of an accuracy estimated from n samples scales as $1/n$, sample support enters the weight automatically. A teacher that survives the filter and is both accurate and well-supported for a class receives a large weight, while a teacher guessing from a few samples is discounted. Our contributions are:

- We present a decentralized, public-data-free FL framework that handles model and data heterogeneity at once: clients of differing architectures collaborate purely through peer distillation over the shared C-dimensional class posterior. Within it, we surface an under-examined problem of how to combine peer teacher predictions, and show that, since teacher reliability is uneven across peers and classes, the usual uniform averaging is a poor choice.
- As our central methodological contribution, we propose CRAD, which, per class, filters out teachers that disagree with the peer consensus and then weights the survivors by the precision (inverse variance) of their class-accuracy estimates. Up to smoothing constants, this precision equals the Fisher information of each estimate, the amount of statistical evidence behind the teacher's competence for that class. It rewards both accuracy and sample support, requires few tuned hyperparameters, and adds only a compact per-class statistics vector to communication.
- On the CIFAR-10, CIFAR-100, and PathMNIST benchmarks, under heterogeneous architectures and non-IID skew, CRAD attains the best global accuracy of all compared methods while maintaining strong local accuracy.

2. Related Work

2.1. Data Heterogeneity in Federated Learning

FL degrades under data heterogeneity, the non-IID data problem [36]. Previous efforts to mitigate this degradation have focused on parameter-space regularization to bound client drift, such as FedProx [19], or variance reduction via control variates, such as SCAFFOLD [15], to stabilize convergence. Another series of works emphasizes model personalization, allowing clients to adapt to local distributions through partial parameter sharing, meta-learning, or personalized objective functions, such as pFedMe [5] and APFL [4]. However, all of these operate within a shared parameter space, whether by global, proximal, or personalized aggregation [7], and so remain incompatible with architecturally distinct models [7, 27], a setting common in practice.

2.2. Knowledge Distillation in Federated Learning

KD sidesteps the homogeneity constraint by transferring knowledge through soft predictions rather than by averaging weight vectors. Predictions stay comparable across architectures over a shared label space [25, 28]. To fuse those predictions into a common target, KD-based federated methods fall into three groups, distinguished by the auxiliary infrastructure they require. The first group aligns clients on a shared public dataset without a central server, distilling each client toward a consensus formed on the common inputs, as in FedMD [18]. This transfers knowledge across architectures but requires a task-relevant public dataset, raising availability and relevance concerns [8]. The second group routes fusion through a central server that distills client predictions into a global consensus and broadcasts it back, as in ensemble distillation [20]. This typically runs on the server's own public or generated data, relocating the dependency rather than removing it, and reintroduces a central coordinator [16, 26]. Recent server-centric variants follow the same pattern. The multi-teacher FedMKD of Sun et al. [29] distills client models into a server-side student with one confidence scalar per teacher, and the personalized FedMKD of Lin et al. [21] initializes each client by blending the global model with the client's own previous-round model in parameter space. Both require a central server and architecturally identical clients. A related self-distillation line [9, 17] selectively distills the global model into the local one, filtering or reweighting its knowledge class by class (and, in [9], sample by sample), but operates within FedAvg, with a single server-aggregated teacher and identical client architectures. The third group needs neither a public dataset nor a central server. Clients distill from one another peer-to-peer over their own data, as in DFML [16] and personalized decentralized KD [12]. Our framework operates

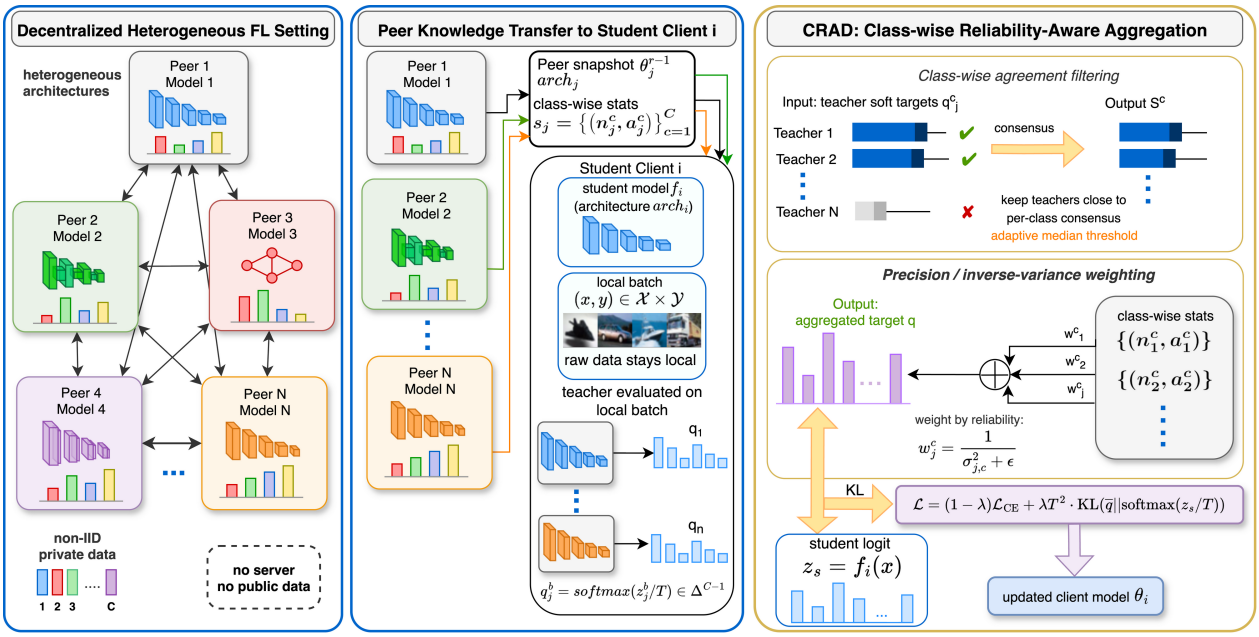


Figure 1. Overview of the proposed CRAD framework. **(1) Decentralized heterogeneous setting:** clients running different architectures collaborate over non-IID private data, with no central server and no public dataset. The only shared interface between any two clients is the C-dimensional class posterior. **(2) Peer knowledge transfer:** a student client receives its peers' model snapshots together with a compact per-class statistics vector, and runs each peer's snapshot on its own local batch to obtain soft predictions q_j, so raw and private data never leaves the client. **(3) Class-wise reliability-aware aggregation:** for each class, CRAD first discards the teachers that disagree with the peer consensus (an adaptive per-class median filter), then combines the survivors by precision (inverse-variance) weighting of their class-accuracy estimates, so that decisive, well-supported teachers dominate the aggregated distillation target $\bar{q}$. The student then updates its model by minimizing a combination of cross-entropy on its local labels and a distillation loss toward this target.

in this regime.

2.3. Combining Teacher Predictions

In most KD-based federated methods, peer predictions are fused by a uniform average over the available teachers [18, 20]. This treats every teacher as equally trustworthy, but teachers trained on different data partitions vary in quality, and their reliability is itself class-dependent. Under non-IID partitions, a given peer may be reliable on its well-represented classes and badly miscalibrated elsewhere. A natural alternative, used in centralized multi-teacher distillation [33], is to weight teachers by prediction confidence or entropy, but confidence is a poor proxy for correctness under distribution shift, and such schemes ignore how much data actually supports each teacher's belief. Reliability-based weighting normally assumes held-out validation data on a trusted server or access to a shared transfer set, neither of which exists in our setting. How to weight teachers by reliability in a fully decentralized, public-data-free, non-IID setting, accounting for the statistical uncertainty of reliability estimated from finite local data, remains largely open. Our work targets this gap. We keep the decentralized, public-data-free KD backbone and present a per-class aggregation that first filters teachers by agreement and then weights each survivor by the precision of its class-accuracy estimate.

3. Method

3.1. Setting and Overview

We consider N clients, each holding a private local dataset $\mathcal{D}_i$ of input-label pairs $(x, y) \in \mathcal{X} \times \mathcal{Y}$ drawn from a client-specific distribution P_i, with a label space $\mathcal{Y} = \{1, \ldots, C\}$ shared across clients. The federation is heterogeneous in two ways at once. The data are non-IID: the class proportions $P_i(y)$ differ sharply across clients, and under severe skew a client may hold few or even no samples of some classes, so its local label set can be a strict subset of $\mathcal{Y}$. The models are heterogeneous: each client i runs a network f_i of its own architecture, scaled to its hardware. These are exactly the conditions under which standard Federated Averaging breaks down: weight averaging is undefined across heterogeneous architectures, and even within one, averaging classifiers trained on skewed partitions can degrade the global model below a local specialist [6, 19, 36].

We therefore discard parameter averaging in favor of fully decentralized, peer-to-peer knowledge distillation, and within it focus on how peer predictions are fused into a dis-

tillation target. The backbone departs from parameter averaging across three coupled dimensions. Rather than averaging in parameter space, knowledge is transferred through soft output distributions produced by teacher models evaluated locally on each client's own data. Rather than requiring architectural uniformity, each client maintains a structurally distinct model. The only interface between teacher and student is the semantically uniform C-dimensional class posterior. Rather than relying on a central server, we operate over a fully connected peer-to-peer topology in which every client communicates directly with all others, with no global coordinator at any stage of training. On top of this backbone, CRAD forms the distillation target through a per-class procedure in two stages: it first discards teachers that disagree with the per-class peer consensus, then combines the survivors with each teacher's contribution scaled by the statistical precision of its class-accuracy estimate. The consensus the student aligns with is thus dominated, for every class, by the teachers that are both in agreement and well-evidenced for it.

3.2. Architecture-Agnostic Knowledge Transfer

At communication round r, each client i maintains its own model f_i and receives a set of model snapshots $\{(\theta_j^{r-1}, \mathrm{arch}_j, \mathbf{s}_j^{r-1})\}_{j\in\mathcal{N}_i}$ from its peers, where $\mathcal{N}_i = \{1,\dots,N\}\setminus\{i\}$ denotes the set of all other clients, arch_j denotes the architecture identifier for client j, and $\mathbf{s}_j^{r-1}$ is a compact class-wise statistics vector defined in Section 3.3. Notably, all clients in round r distill from round $r-1$ snapshots. For each training batch $(x^{(b)}, y^{(b)})$ sampled from $\mathcal{D}_i$, client i instantiates each neighbor's architecture $f_{\theta_j^{r-1}}$ locally and computes the teacher logits:

$$z_j^{(b)} = f_{\theta_j^{r-1}}(x^{(b)}), \quad j \in \mathcal{N}_i, \tag{1}$$

followed by a temperature-scaled softmax ($T > 0$) that softens the distribution [10], yielding the soft target vector $q_j^{(b)}$:

$$q_j^{(b)} = \mathrm{softmax}(z_j^{(b)}/T) \in \Delta^{C-1}, \tag{2}$$

where Δ^{C-1} denotes the probability simplex over C classes. The soft target $q_j^{(b)}$ encodes what neighbor j believes about the class structure of the student's own local sample $x^{(b)}$, including classes the student may have never encountered. This is the mechanism by which knowledge of unseen classes propagates across the network without a shared dataset or central coordinator. Because teacher inference runs entirely on the student's data, no raw samples leave the client. Because each teacher functions as a black-box mapping $x \to \mathbb{R}^C$, any two models sharing the same label space $\mathcal{Y}$ are mutually compatible for knowledge transfer regardless of their internal architecture.

3.3. Class-wise Reliability-Aware Aggregation

Given the per-teacher soft targets $\{q_j^{(b)}\}_{j\in\mathcal{N}_i}$ of Eq. 2, the remaining question is how to combine them into a single distillation target. The standard choice is the uniform mean over all peers [20],

$$\bar{q}_{\mathrm{unif}}^{(b)} = \frac{1}{|\mathcal{N}_i|}\sum_{j\in\mathcal{N}_i} q_j^{(b)}, \tag{3}$$

which weights every teacher equally for every class. This is wasteful under heterogeneity. A teacher's competence is class-dependent, likely high for classes it has seen often and low for classes it has seen rarely or never. We instead operate separately for each class in two stages: we first discard teachers that lack support for the class or disagree with the per-class peer consensus, then aggregate the survivors weighted by an estimate of their reliability for that class.

Class-wise agreement filtering. Before weighting, we first drop, for each class, teachers whose local class support falls below a per-class threshold $n_{\min}^c$, set to a quantile of the peers' support counts $\{n_j^c\}_{j\in\mathcal{N}_i}$ (see Table 1 caption), defining a competent teacher subset $\mathcal{N}_i^c = \{\, j \in \mathcal{N}_i : n_j^c \geq n_{\min}^c \,\}$. Among these remaining teachers, we then discard those whose predictions deviate most from the peer consensus on that class. To this end, we form a preliminary per-class consensus and measure each teacher's deviation from it,

$$\tilde{q}^c = \frac{1}{|\mathcal{N}_i^c|}\sum_{j\in\mathcal{N}_i^c} q_j^c, \qquad d_j^c = \left|\, q_j^c - \tilde{q}^c \,\right|, \tag{4}$$

and retain for each class the teachers whose deviation is at most the median deviation for that class,

$$\tau_c = \underset{j\in\mathcal{N}_i^c}{\mathrm{median}}\, d_j^c, \qquad \mathcal{S}_i^c = \left\{\, j \in \mathcal{N}_i^c \;:\; d_j^c \leq \tau_c \,\right\}. \tag{5}$$

This adaptive, per-class median retains the supported teachers most in agreement with the consensus and introduces no threshold to tune. The class-wise aggregation below then ranges over $\mathcal{S}_i^c$ rather than the full peer set, and different classes may draw on different teacher subsets.

Class-wise reliability statistics. Alongside its snapshot, each client j shares a compact statistics vector $\mathbf{s}_j = \{(n_j^c, a_j^c)\}_{c=1}^C$ recording, for each class c, its class-c accuracy a_j^c, evaluated with its current model on a held-out validation split of its own shard, and the number n_j^c of class-c examples in that split, on which the accuracy is computed. This is $2C$ scalars per client per round, negligible compared to the model weights, and exposes no raw samples.

Reliability as a statistical estimate. The accuracy a_j^c is a noisy signal: the same value is more credible when measured on many class-c examples than on a handful. We therefore treat a_j^c as a Bernoulli proportion over the n_j^c examples it was measured on, applying the Agresti–Coull correction to stabilize small-sample estimates and taking its associated variance,

$$\tilde{a}_j^c = \frac{a_j^c\, n_j^c + 2}{n_j^c + 4}, \qquad \sigma_{j,c}^2 = \frac{\tilde{a}_j^c\,(1-\tilde{a}_j^c)}{n_j^c + 4}. \tag{6}$$

Inverse-variance (precision) weighting. We weight each surviving teacher by the precision (inverse variance) of its class-accuracy estimate. The weight rises with both the decisiveness of the estimated accuracy and the amount of evidence behind it (up to the Agresti–Coull smoothing constants, the precision equals the Fisher information of the estimate). Precision is the standard rule for combining estimates of differing reliability [3]. Because precision accrues linearly with additional samples, a teacher's influence grows in proportion to its evidence. Weights not proportional to $1/\sigma^2$ break this proportionality, and every alternative we tested performs worse (Tab. 4). We thus set the class-wise weight

$$w_j^c = \frac{1}{\sigma_{j,c}^2 + \epsilon}, \tag{7}$$

where $\epsilon > 0$ guards against division by zero. We aggregate the surviving teachers class by class as a precision-weighted average:

$$\overline{q}^c = \frac{\sum_{j \in \mathcal{S}_i^c} w_j^c\, q_j^c}{\sum_{j \in \mathcal{S}_i^c} w_j^c + \epsilon}, \qquad \overline{q} \leftarrow \frac{\overline{q}}{\sum_{c=1}^{C} \overline{q}^c}, \tag{8}$$

where $\mathcal{S}_i^c$ is the agreement-filtered teacher set of Eq. 5 and the renormalization restores $\overline{q}$ to the probability simplex (we omit the batch index b on $\overline{q}^c$, q_j^c for brevity). The weight is a per-class trust score on the teacher's predictions. Precision alone rewards decisiveness rather than correctness, so the weighting is applied only after the class-wise filter removes teachers with insufficient support or predictions that substantially deviate from the peer consensus. Under the standard assumption that unreliable or outlying teachers constitute a minority, this filtering reduces the risk that a confidently inaccurate teacher receives a high weight. A teacher is trusted for a class to the degree that it is confident, well-evidenced, and in consensus. That said, repeated mutual distillation couples the teachers across rounds, so their predictions are not independent. We use the weight as a trust score rather than as a minimum-variance combiner, for which independence would be required.

Overall, the training objective balances local cross-entropy supervision, $\mathcal{L}_{\mathrm{CE}}$, with a distillation term that aligns the student's predictions with the precision-weighted consensus:

$$\mathcal{L} = (1-\lambda)\,\mathcal{L}_{\mathrm{CE}} + \lambda\, T^2 \cdot \mathrm{KL}\left(\overline{q} \,\|\, \mathrm{softmax}(z_s/T)\right), \tag{9}$$

where $z_s = f_i(x^{(b)})$ is the student's own logit vector and $\lambda \in [0,1]$ is the distillation weight, balancing reliance on the peer consensus against the local ground-truth labels. The temperature-scaled KL term with its T^2 factor is the standard distillation objective, here applied to the aggregated target $\overline{q}$ rather than to a single teacher. Algorithm 1 summarizes the complete CRAD framework.

4. Experiments

4.1. Experimental Setup

Datasets and Partitioning. We evaluate the proposed framework on three benchmarks from distinct domains: CIFAR-10 and CIFAR-100 for natural-image classification, and PathMNIST [32] for colon-pathology histology. PathMNIST comprises nine tissue classes from the MedMNIST collection and represents a realistic, privacy-sensitive medical setting. Each dataset is partitioned across $N = 10$ clients (unless otherwise specified) under a Dirichlet distribution with concentration parameter $\alpha = 0.3$. This induces severe label skew. These public benchmarks serve only to construct the simulated federation: each client trains on its own private shard alone, and the method uses no shared or public data.

Architecture Pool. To validate architectural heterogeneity, the framework uses three structurally distinct models: ResNet-18 ($\approx$ 11M parameters), ResNet-18-Half ($\approx$ 2.8M parameters, $0.5\times$ channel scaling), and a plain CNN ($\approx$ 0.8M parameters, 2 conv + 2 FC). This pool evaluates both width heterogeneity, through the channel scaling between the ResNet variants, and family heterogeneity, through the absence of residual connections in the plain CNN. Architectures are assigned deterministically across the 10 clients via a round-robin schedule, denoted as $\mathrm{arch}_i = \mathrm{POOL}[i \bmod 3]$. This capacity heterogeneity, combined with the non-IID skew, makes teacher reliability uneven and class-dependent, reflecting common real-world deployment scenarios.

Compared Methods. All methods are evaluated under the same heterogeneous architecture pool, non-IID partition, and training schedule. We compare against five representative heterogeneous-FL distillation baselines that span the auxiliary-component taxonomy of Section 2. FedMD [18] aligns clients on a shared public proxy dataset (size 500) before local adaptation, directly testing the value of our public-data-free design. FedGD [34] replaces the public proxy with a synthetic transfer set (size 500) generated rather than collected, a data-free variant of the

Algorithm 1: Class-wise Reliability-Aware Distillation (CRAD)

Input : N clients with local datasets $\{\mathcal{D}_i\}_{i=1}^{N}$, temperature T, loss weight λ, smoothing constant ϵ
Output: Updated client models $\{f_{\theta_i}\}_{i=1}^{N}$
Initialize model f_{θ_i} for all clients $i \in \{1, \ldots, N\}$;
for *each communication round* $r = 0$ *to* $R-1$ **do**
  Freeze current models as snapshots: $\theta_{\text{prev},i} \leftarrow \theta_i$ for all i;
  Each client computes class statistics $\mathbf{s}_i = \{(n_i^c, a_i^c)\}_{c=1}^{C}$ (validation count n_i^c, validation accuracy a_i^c);
  for *each client* $i = 1$ *to* N **do**
    Define peer set $\mathcal{N}_i = \{1, \ldots, N\} \setminus \{i\}$ and, per class, the support-filtered subset $\mathcal{N}_i^c \subseteq \mathcal{N}_i$ of teachers with sufficient class-c samples;
    Compute precision weights from peer statistics: $\tilde{a}_j^c = \frac{a_j^c n_j^c + 2}{n_j^c + 4}$, $\sigma_{j,c}^2 = \frac{\tilde{a}_j^c(1-\tilde{a}_j^c)}{n_j^c+4}$, $w_j^c = \frac{1}{\sigma_{j,c}^2 + \epsilon}$, $\forall j \in \mathcal{N}_i, c$;
    for *each batch* $(x, y) \in \mathcal{D}_i$ **do**
      Student logits and cross-entropy loss: $z_s = f_{\theta_i}(x)$, $\mathcal{L}_{\text{CE}} = \text{CE}(z_s, y)$;
      Compute teacher soft targets (no gradients): $q_j = \text{Softmax}(f_{\theta_{\text{prev},j}}(x)/T), \quad \forall j \in \mathcal{N}_i$;
      Class-wise agreement filter (adaptive per-class median), over $\mathcal{N}_i^c$: $\tilde{q}^c = \frac{1}{|\mathcal{N}_i^c|}\sum_{j \in \mathcal{N}_i^c} q_j^c$, $\tau^c = \text{median}_{j \in \mathcal{N}_i^c} |q_j^c - \tilde{q}^c|$, $\mathcal{S}^c = \{j \in \mathcal{N}_i^c : |q_j^c - \tilde{q}^c| \le \tau^c\}$;
      Filtered precision-weighted class-wise aggregate: $\overline{q}^c = \frac{\sum_{j \in \mathcal{S}^c} w_j^c q_j^c}{\sum_{j \in \mathcal{S}^c} w_j^c + \epsilon}$, then normalize $\overline{q} \leftarrow \overline{q} / \sum_c \overline{q}^c$;
      KD and total loss: $\mathcal{L}_{\text{KD}} = T^2 \cdot \text{KL}(\overline{q} \,\|\, \text{Softmax}(z_s/T))$, $\mathcal{L} = (1-\lambda)\mathcal{L}_{\text{CE}} + \lambda \mathcal{L}_{\text{KD}}$;
      Update θ_i via backpropagation (with gradient clipping);

same public-data paradigm. MSFKD [30] is a multi-teacher selective federated distillation method. DFML [16] is the closest baseline to our backbone, a fully decentralized, public-data-free, peer-to-peer mutual distillation method that, like ours, exchanges no raw data and uses no server, but fuses peers without class-wise reliability weighting. FedMKD [21] is a recent multi-teacher method that reuses each client's own previous-round model as an additional teacher. Its implementation is not public, so we adapt it to our decentralized, architecture-heterogeneous setting. Within our framework, the central comparison isolates the effect of teacher aggregation. We compare CRAD against two aggregation variants: Uniform KD, the conventional uniform average (Eq. 3); and Uncertainty KD, which weights teachers by the negative entropy of their predictions.

Training Protocol. Each client is trained for $R = 300$ communication rounds, one local epoch per round, with the distillation weight $\lambda = 0.7$ and a random seed of 1024. Each client's held-out partition is split evenly into a validation half and a test half. The validation half supplies the reliability statistics of Section 3.3 and selects the checkpoint. The test half is touched only for final reporting. We report two metrics: global accuracy on each benchmark's standard test set, never used during training or model selection (our primary metric, measuring generalization), and local accuracy on each client's held-out test half (measuring local adaptation). Because a client can score high local accuracy simply by overfitting the classes it holds, local accuracy serves mainly as a guardrail, confirming that global-accuracy gains do not come at a large cost in local adaptation. For every method, both metrics are reported at the round with the highest average local validation accuracy.

4.2. Experimental Results

Table 1 reports all methods on all three benchmarks under identical conditions.

CIFAR-10. The three aggregation variants are comparable on local accuracy, consistent with its guardrail role. They differ chiefly on global accuracy, which draws on borrowed knowledge of rarely-seen classes. There CRAD leads at 78.60%, ahead of Uncertainty KD (77.41%) and the uniform average (77.19%). Uncertainty KD barely improves on uniform averaging because confidence is a weak proxy for correctness under distribution shift, whereas CRAD's agreement filter keeps only teachers that align with the peer consensus, and its precision weight then favors those whose class beliefs are both decisive and well-supported. All competing methods trail our framework in global accuracy. FedMKD [21] is the strongest at 74.54%, still four points below CRAD. The public-data methods FedMD, MSFKD and FedGD are limited by the quality of their proxy or synthetic transfer set. DFML (61.99%), the decentralized public-data-free method closest to our backbone, trails here, although it is the strongest competitor on

Table 1. Teacher-aggregation comparison on CIFAR-10, CIFAR-100, and PathMNIST ($N = 10$, non-IID Dirichlet, $R = 300$). All decentralized-KD methods share the same backbone and distillation weight $\lambda = 0.7$, differing only in how peer teachers are combined. The checkpoint is selected on each client's validation split. CRAD's support threshold $n^c_{\min}$ is the per-class peer median on CIFAR-10 and CIFAR-100, and the 20th percentile on PathMNIST. Accuracies are percentages, with global accuracy the primary metric. Best aggregation result in each column in **bold**.

	CIFAR-10		CIFAR-100		PathMNIST	
Method	Global	Local	Global	Local	Global	Local
Competing heterogeneous-FL methods						
FedMD [18]	71.69	86.96	36.23	55.85	86.58	88.04
FedGD [34]	67.87	86.48	30.50	50.80	82.86	86.93
MSFKD [30]	69.22	86.44	32.77	50.63	62.19	72.04
DFML [16]	61.99	66.88	47.29	54.12	70.40	74.06
FedMKD [21]	74.54	87.30	38.05	55.59	88.35	87.65
Our framework, varying teacher aggregation						
Uniform KD	77.19	87.73	41.53	58.54	87.59	87.89
Uncertainty KD	77.41	**87.87**	42.06	58.74	86.41	87.09
CRAD (Ours)	**78.60**	87.09	**48.22**	**59.87**	**89.44**	**88.14**

CIFAR-100. That every aggregation variant in our framework exceeds every competing method isolates the contribution of the decentralized backbone, while the gap between CRAD and Uniform KD isolates that of reliability-aware aggregation.

Scaling to More Classes (CIFAR-100). The CIFAR-100 columns of Table 1 cover a 100-class benchmark in which each client holds far fewer samples per class, stressing the reliability estimates that drive CRAD. On this harder benchmark, CRAD again ranks first, at 48.22% global accuracy, ahead of the strongest competitor DFML (47.29%) and well above the uniform average (41.53%) and Uncertainty KD (42.06%). Two patterns stand out: the margin over uniform averaging widens sharply relative to CIFAR-10, from about one point to nearly seven, and DFML now overtakes the uniform and uncertainty-based variants that outscored it on CIFAR-10. Both follow from the same cause. With 100 classes and far fewer samples per class, per-class beliefs are noisier and locally-rare classes more numerous, the regime in which tying a teacher's weight to its reliability pays off.

Consistency on a Medical Benchmark. PathMNIST instantiates the clinical scenario of Section 1: sensitive slides that sites cannot share, held at institutions running widely differing hardware. Its columns in Table 1 show CRAD again attaining the best global accuracy (89.44%, against 87.59% for the uniform average) and the best local accuracy (88.14%). That the gain transfers from natural images to histopathology indicates that reliability-aware aggregation is not specific to one data domain.

Table 2. Cost on CIFAR-10 ($N = 10$), measured during the runs of Table 1 with every method on the same machine (specified in Appendix A.5). Payload is what one client transmits per round, Time the wall-clock duration of a full communication round, and GPU Mem. its peak allocated GPU memory. "Proxy" marks methods additionally requiring public or synthetic data.

Method	Payload (MB)	Time (s)	GPU Mem. (GB)	Proxy
Competing heterogeneous-FL methods				
FedMD [18]	0.38	37.6	1.38	yes
FedGD [34]	0.04	26.2	3.33	yes
MSFKD [30]	0.04	25.1	1.57	yes
DFML [16]	38.9	53.8	1.20	no
FedMKD [21]	194.3	46.1	1.56	no
Our framework, varying teacher aggregation				
Uniform KD	194.3	20.6	0.60	no
Uncertainty KD	194.3	20.0	0.60	no
CRAD (Ours)	194.3	21.3	0.60	no

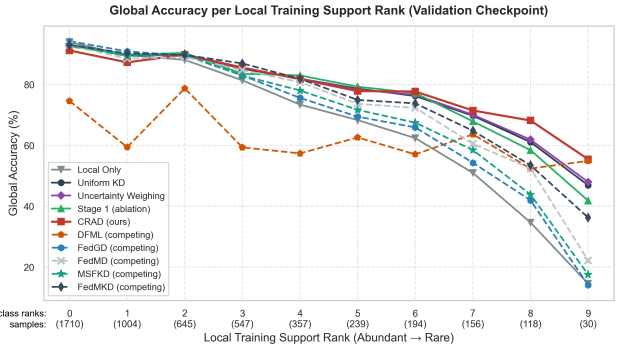


Figure 2. Per-class global accuracy on CIFAR-10 with classes ordered by local training support (shown in parentheses, abundant to rare), for all compared methods. The methods agree more on well-supported classes and separate on the rare ones, where CRAD degrades the least.

4.3. Analyses

Per-Class Gains. Figure 2 breaks global accuracy down by class, ordered from abundant to rare local support. On a class that a client holds few samples of, the uniform average dilutes the few competent teachers among a majority of uninformed ones, and a teacher can be confidently wrong on a class it has never seen. Tying the weight to the teacher's reliability down-weights the uninformed ones. The figure bears this out: the methods are nearly indistinguishable where support is plentiful and separate as it dwindles. On the rarest class (30 local samples), CRAD retains about 56% accuracy against about 47% for the other aggregation variants, and it leads every competing method on the five rarest classes. The Stage-1 ablation, CRAD's agree-

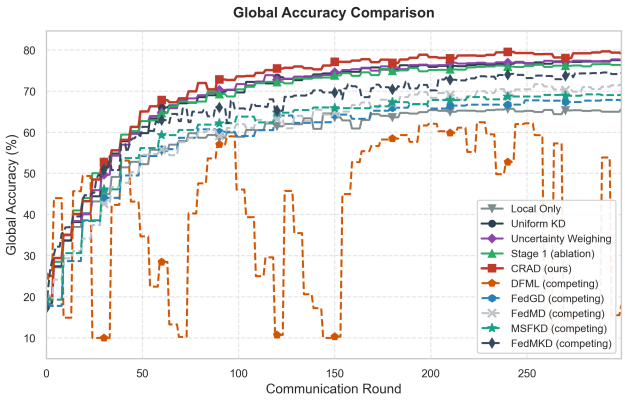


Figure 3. Global accuracy vs. communication round for all compared methods on CIFAR-10. CRAD (red) stays above every other method from the early rounds onward and converges stably, whereas DFML swings sharply from round to round.

ment filter without the precision weight, does no better than the uniform average on these rare classes, so the lift comes mainly from precision-weighting the survivors, not from the filter alone.

Convergence and Stability. Figure 3 plots global accuracy over communication rounds. CRAD sits above every baseline, including the Stage-1 ablation, from the early rounds onward and converges smoothly, whereas DFML's curve swings sharply round to round, so the round selected on validation sits far above its typical accuracy.

Communication, Compute, and Memory Cost. Table 2 shows that cost is set by the regime, not by the aggregation rule. Proxy-based methods communicate only predictions over the transfer set and are cheap, but require that set to exist, whereas every snapshot-based decentralized method exchanges full snapshots. Within that regime, CRAD's own overhead is the $2C$-scalar statistics vector, under 1 KB, and it completes a round faster and at lower peak memory than every competing method. Round time and peak memory are both dominated by holding and running the $N-1$ peer teachers, hence nearly identical across our three aggregation variants. The higher payload is the price of requiring neither public data nor a server.

Client-Number Ablation. To test scalability under sparse participation, we grow the pool to $N \in \{20, 50, 100\}$ clients while activating 10 per round. As shown in Table 3, CRAD improves both global and local accuracy over Uniform KD at every pool size, and its relative advantage widens as the pool grows, from a factor of 1.2 on global accuracy at N=20 to 2.0 at N=100. This suggests that

Table 3. Client-number ablation on CIFAR-10 with partial participation. Each run uses $R = 300$ rounds and activates 10 clients per round. Accuracies are averaged over all clients.

	N=20		N=50		N=100	
Method	Global	Local	Global	Local	Global	Local
Uniform KD	53.77	68.89	22.81	54.02	11.01	40.83
CRAD (Ours)	**64.18**	**72.58**	**29.94**	**58.16**	**22.19**	**55.83**

Table 4. Ablation of teacher-weighting rules on CIFAR-100. All variants use the same CRAD framework and differ only in the aggregation weight. Acc.: accuracy-only; Sup.: support-only; SM: $\mathrm{softmax}(-\sigma^2)$; LCB: $\max(0, \tilde{a} - \sigma)$; CE: cross-entropy.

	$1/\sigma$	Acc.	Sup.	SM	LCB	$1/\mathrm{CE}$	**CRAD**
Global Acc.	46.89	47.22	47.25	46.71	47.02	47.17	**48.22**
Local Acc.	57.98	58.56	58.26	58.45	58.54	58.53	**59.87**

CRAD is particularly effective under sparse participation, where teacher quality varies more widely.

Weighting Rule. Table 4 swaps the precision weight for six alternatives on CIFAR-100, holding the rest of CRAD fixed. Precision weighting is best on both metrics. Accuracy alone and support alone each capture part of the gain, but combining them via precision weighting beats either. Weighting by $1/\sigma$ rather than $1/\sigma^2$ is the weakest variant on local accuracy, consistent with precision being the scale on which evidence adds (Sec. 3.3).

5. Limitations and Future Work

CRAD requires sharing a per-class statistics vector, which reveals each client's validation label proportions through the counts n_j^c. These are fixed across rounds, so a single noised release suffices and its privacy cost does not compose over rounds. The counts have L_1-sensitivity one under record add/remove adjacency, so Laplace noise of scale $1/\varepsilon$ gives ε-differential privacy. At $\varepsilon = 1$, this costs 0.82 points of global accuracy on CIFAR-100 (48.22% vs. 47.40%), still ahead of every competing method in Table 1. End-to-end differential privacy covering the snapshots remains open and is left to future work.

6. Conclusion

We presented a decentralized, server-free, public-data-free framework in which architecturally heterogeneous clients collaborate purely through peer distillation, and proposed CRAD, a per-class aggregation that filters teachers by consensus agreement and weights the survivors by the precision of their class-accuracy estimates. Across CIFAR-10/100 and PathMNIST under heterogeneous architectures and severe non-IID skew, CRAD attains the best global accuracy.

References

[1] Farzam Asad, Junaid Saif Khan, Maria Tariq, Sundus Munir, and Muhammad Adnan Khan. Federated proximal optimization for privacy-preserving heart disease prediction: A controlled simulation study on non-IID clinical data. *arXiv preprint arXiv:2601.17183*, 2026. 1

[2] Christopher Briggs, Zhong Fan, and Peter Andras. Federated learning with hierarchical clustering of local updates to improve training on non-IID data. In *Proceedings of the International Joint Conference on Neural Networks (IJCNN)*, pages 1–9, 2020. 1

[3] William G. Cochran. The combination of estimates from different experiments. *Biometrics*, 10(1):101–129, 1954. 5

[4] Yuyang Deng, Mohammad Mahdi Kamani, and Mehrdad Mahdavi. Adaptive personalized federated learning. *arXiv preprint arXiv:2003.13461*, 2020. 2

[5] Canh T. Dinh, Nguyen H. Tran, and Tuan D. Nguyen. Personalized federated learning with Moreau envelopes. In *Proceedings of the Conference on Neural Information Processing Systems (NeurIPS)*, pages 21394–21405, 2020. 2

[6] Alireza Fallah, Aryan Mokhtari, and Asuman Ozdaglar. Personalized federated learning with theoretical guarantees: A model-agnostic meta-learning approach. In *Proceedings of the Conference on Neural Information Processing Systems (NeurIPS)*, pages 3557–3568, 2020. 3

[7] Boyu Fan, Siyang Jiang, Xiang Su, Sasu Tarkoma, and Pan Hui. A survey on model-heterogeneous federated learning: Problems, methods, and prospects. In *Proceedings of the IEEE International Conference on Big Data (BigData)*, pages 7725–7734, 2024. 1, 2

[8] Cheng Guo, Qianqian He, Xinyu Tang, Yining Liu, and Yingmo Jie. Parameterized data-free knowledge distillation for heterogeneous federated learning. *Knowledge-Based Systems*, 317:113502, 2025. 1, 2

[9] Yuting He, Yiqiang Chen, Xiaodong Yang, Hanchao Yu, Yi-Hua Huang, and Yang Gu. Learning critically: Selective self-distillation in federated learning on non-IID data. *IEEE Transactions on Big Data*, 10(6):789–800, 2024. 2

[10] Geoffrey Hinton, Oriol Vinyals, and Jeff Dean. Distilling the knowledge in a neural network. *arXiv preprint arXiv:1503.02531*, 2015. 4

[11] Sohei Itahara, Takayuki Nishio, Yusuke Koda, Masahiro Morikura, and Koji Yamamoto. Distillation-based semi-supervised federated learning for communication-efficient collaborative training with non-IID private data. *IEEE Transactions on Mobile Computing*, 22(1):191–205, 2023. 1

[12] Eunjeong Jeong and Marios Kountouris. Personalized decentralized federated learning with knowledge distillation. *arXiv preprint arXiv:2302.12156*, 2023. 2

[13] Daniel M. Jimenez-Gutierrez, Mehrdad Hassanzadeh, Aris Anagnostopoulos, Ioannis Chatzigiannakis, and Andrea Vitaletti. A thorough assessment of the non-IID data impact in federated learning. *arXiv preprint arXiv:2503.17070*, 2025. 1

[14] Peter Kairouz et al. Advances and open problems in federated learning. *Foundations and Trends in Machine Learning*, 14(1–2):1–210, 2021. 1

[15] Sai Praneeth Karimireddy, Satyen Kale, Mehryar Mohri, Sashank J. Reddi, Sebastian U. Stich, and Ananda Theertha Suresh. SCAFFOLD: Stochastic controlled averaging for federated learning. In *Proceedings of the International Conference on Machine Learning (ICML)*, pages 5132–5143, 2020. 1, 2

[16] Yasser H. Khalil, Amir H. Estiri, Mahdi Beitollahi, Nader Asadi, Sobhan Hemati, Xu Li, Guojun Zhang, and Xi Chen. DFML: Decentralized federated mutual learning. arXiv preprint arXiv:2402.01863, 2024. 1, 2, 6, 7

[17] Gihun Lee, Minchan Jeong, Yongjin Shin, Sangmin Bae, and Se-Young Yun. Preservation of the global knowledge by not-true distillation in federated learning. In *Advances in Neural Information Processing Systems (NeurIPS)*, 2022. 2

[18] Daliang Li and Junpu Wang. FedMD: Heterogeneous federated learning via model distillation. *arXiv preprint arXiv:1910.03581*, 2019. 1, 2, 3, 5, 7

[19] Tian Li, Anit Kumar Sahu, Manzil Zaheer, Maziar Sanjabi, Ameet Talwalkar, and Virginia Smith. Federated optimization in heterogeneous networks. In *Proceedings of Machine Learning and Systems (MLSys)*, pages 429–450, 2020. 1, 2, 3

[20] Tao Lin, Lingjing Kong, Sebastian U. Stich, and Martin Jaggi. Ensemble distillation for robust model fusion in federated learning. In *Proceedings of the Conference on Neural Information Processing Systems (NeurIPS)*, pages 2351–2363, 2020. 1, 2, 3, 4

[21] Tianjia Lin, Zhou Tan, and Ximeng Liu. FedMKD: Personalized federated learning with memory knowledge distillation. In *IEEE International Conference on Communications (ICC)*, pages 4945–4950, 2025. 2, 6, 7

[22] Grigory Malinovsky, Samuel Horváth, Konstantin Burlachenko, and Peter Richtárik. Federated learning with regularized client participation. *arXiv preprint arXiv:2302.03662*, 2023. 1

[23] H. Brendan McMahan and Daniel Ramage. Federated learning: Collaborative machine learning without centralized training data, 2017. Google AI Blog. 1

[24] H. Brendan McMahan, Eider Moore, Daniel Ramage, Seth Hampson, and Blaise Agüera y Arcas. Communication-efficient learning of deep networks from decentralized data. In *Proceedings of the 20th International Conference on Artificial Intelligence and Statistics (AISTATS)*, pages 1273–1282, 2017. 1

[25] Alessio Mora, Irene Tenison, Paolo Bellavista, and Irina Rish. Knowledge distillation in federated learning: A practical guide. In *Proceedings of the Thirty-Third International Joint Conference on Artificial Intelligence (IJCAI)*, pages 8188–8196, 2024. 1, 2

[26] Tuc Van Nguyen, Mark A. Dakka, Sonya M. Diakiw, Matthew D. VerMilyea, Michelle Perugini, Jonathan M. M. Hall, and Don Perugini. A novel decentralized federated learning approach to train on globally distributed, poor quality, and protected private medical data. *Scientific Reports*, 12 (1):8888, 2022. 1, 2

[27] Kilian Pfeiffer, Martin Rapp, Ramin Khalili, and Jörg Henkel. Federated learning for computationally-constrained

heterogeneous devices: A survey. *ACM Computing Surveys*, 55(14s):1–27, 2023. 1, 2

[28] Hassan Salman, Chamseddine Zaki, Nour Charara, Sonia Guehis, Jean-François Pradat-Peyre, and Abbass Nasser. Knowledge distillation in federated learning: A comprehensive survey. *Discover Computing*, 28(1):145, 2025. 2

[29] Huifang Sun, Jiaming Pei, Xiaoqing Xu, Rubing Xue, Lingyun Zhao, Qihang Sun, Longfei Li, and Lukun Wang. FedMKD: Multi-teacher knowledge distillation for communication-efficient federated learning. *Cluster Computing*, 28:638, 2025. 2

[30] Dong Wang, Naifu Zhang, Meixia Tao, and Xu Chen. Knowledge selection and local updating optimization for federated knowledge distillation with heterogeneous models. *IEEE Journal of Selected Topics in Signal Processing*, 17(1): 82–97, 2023. 6, 7

[31] Jianyu Wang, Qinghua Liu, Hao Liang, Gauri Joshi, and H. Vincent Poor. Tackling the objective inconsistency problem in heterogeneous federated optimization. In *Proceedings of the Conference on Neural Information Processing Systems (NeurIPS)*, pages 7611–7623, 2020. 1

[32] Jiancheng Yang et al. MedMNIST v2 – A large-scale lightweight benchmark for 2D and 3D biomedical image classification. *Scientific Data*, 10(1):41, 2023. 5

[33] Hailin Zhang, Defang Chen, and Can Wang. Confidence-aware multi-teacher knowledge distillation. In *Proceedings of the IEEE International Conference on Acoustics, Speech and Signal Processing (ICASSP)*, pages 4498–4502, 2022. 3

[34] Jie Zhang, Chen Chen, Weiming Zhuang, and Lingjuan Lyu. Target: Federated class-continual learning via exemplar-free distillation. In *Proceedings of the IEEE/CVF International Conference on Computer Vision*, pages 4782–4793, 2023. 5, 7

[35] Yingqi Zhang, Hui Xia, Shuo Xu, Xiangxiang Wang, and Lijuan Xu. AdaptFL: Adaptive federated learning framework for heterogeneous devices. *Future Generation Computer Systems*, 165:107610, 2025. 1

[36] Yue Zhao, Meng Li, Liangzhen Lai, Naveen Suda, Damon Civin, and Vikas Chandra. Federated learning with non-IID data. *arXiv preprint arXiv:1806.00582*, 2018. 1, 2, 3

This appendix is organized as follows: Appendix A specifies optimization settings, hyperparameters, the support pre-filter, evaluation conventions, and the compute environment. Appendix B provides a qualitative view of how CRAD forms its per-class distillation target on individual test images, including a case where the mechanism fails. It uses the same CIFAR-10 run as Table 1, read at the same best-validation checkpoint.

A. Extended Implementation and Hyperparameter Details

A.1. Hyperparameter Summary

Table 5 summarizes the exact hyperparameter values across all three benchmark datasets (CIFAR-10, CIFAR-100, and PathMNIST).

A.2. Validation Splitting

Each client's partitioned evaluation set is split 50/50 into a dedicated local validation split and an untouched local test split. The validation split is used only for computing local empirical validation accuracies a_j^c, class sample counts n_j^c, and checkpoint selection.

A.3. Support Pre-Filtering

Before the Stage-1 agreement filter and Stage-2 precision weighting, peers lacking sufficient local support for class c are pruned by the support cutoff $n_{\min}^c$. On CIFAR-10 and CIFAR-100, $n_{\min}^c$ is set to the peer median, retaining the top 50% of peers with the highest local class support. On PathMNIST, which exhibits higher class density, $n_{\min}^c$ is set to the 20th percentile, retaining the top 80% of peers by local class support.

A.4. Checkpoint Selection and Evaluation Metrics

- **Validation-Based Checkpoint Selection:** Following standard federated learning protocol, the checkpoint is selected using validation performance rather than test performance. At each round, each client evaluates its model on its local validation split. The round achieving the highest unweighted mean validation accuracy across all $N = 10$ clients is selected as the optimal checkpoint: Round 228 for CIFAR-10, Round 277 for CIFAR-100, and Round 285 for PathMNIST.
- **Global Accuracy:** The model snapshots saved at the selected optimal round are evaluated individually on the official benchmark test set (10,000 samples for CIFAR-10/CIFAR-100; 7,180 samples for PathMNIST). The reported accuracy is the unweighted macro-average over all N client models, rather than an ensemble evaluation.

A.5. Compute Environment

Every experiment used a single NVIDIA A100-SXM4-80GB GPU on the Cheaha high-performance computing cluster at the University of Alabama at Birmingham, with 6 AMD EPYC CPU cores and 60 GB of host memory allocated per job. The software stack was PyTorch 2.6.0, CUDA 12.4, and Python 3.11.4 on Linux. The timing and memory figures in Table 2 come from the same runs as the accuracy figures in Table 1, all executed under this configuration. GPU Mem. reports the peak GPU memory allocated during each run.

B. Qualitative Mechanism on Individual Images

The per-class breakdown in Fig. 2 shows which classes reliability-aware aggregation helps on, averaged over clients and test images. They do not show how the two stages act on any single prediction. Figure 5 resolves one

Table 5. **Comprehensive Hyperparameter Configuration.** Parameters used in the experimental benchmark runs for CRAD across CIFAR-10, CIFAR-100, and PathMNIST.

Category	Hyperparameter	CIFAR-10	CIFAR-100	PathMNIST
Local Training	Local Optimizer	SGD	SGD	SGD
	Initial Learning Rate	0.1	0.1	0.1
	Momentum	0.9	0.9	0.9
	Weight Decay	5×10^{-4}	5×10^{-4}	5×10^{-4}
	Learning Rate Decay ($\times 0.99$/round)	Exponential	Exponential	Exponential
	Local Batch Size	64	64	64
	Communication Rounds (R)	300	300	300
	Local Epochs per Round	1	1	1
Distillation (CRAD)	Distillation Temperature (T)	4.0	4.0	4.0
	Distillation Weight (λ)	0.7	0.7	0.7
	Support Threshold ($n^c_{\min}$)	Top 50%	Top 50%	Top 80%
	Agreement Filter Cutoff (τ_c)	Median Deviation	Median Deviation	Median Deviation
	Variance Numerical Guard (ϵ)	10^{-6}	10^{-6}	10^{-6}
Splits & Checkpoints	Local Evaluation Split Protocol	50/50 val/test	50/50 val/test	50/50 val/test
	Local Validation Samples per Client	≈ 500	≈ 530	≈ 361
	Checkpoint Selection Criterion	Mean Local Val.	Mean Local Val.	Mean Local Val.

success case and one failure case down to the individual teacher.

Setup. Figure 4 gives the context that drives the weights. Panel (a) is the per-client validation support n^c_j under the Dirichlet (α=0.3) partition, the count that enters the variance of Eq. 6 through Agresti–Coull smoothing. Panel (b) is the per-client accuracy on the balanced global test set, broken down by class. The two are related but not identical, which is the reason CRAD weights on both accuracy and the evidence behind it rather than on either alone.

Clients are labeled by architecture, with RN18, RN18/2, and CNN6 denoting ResNet-18, ResNet-18-Half, and the plain CNN of Sec. 4.

The two panels of Fig. 5 trace one test image each. For every client we report the assigned distillation weight W, that is the precision weight of Eq. 7 after per-class normalization, and in parentheses the probability that client assigns to the true class. Clients are marked in one of three states: retained and weighted, dropped for insufficient class support, or dropped as a consensus outlier. The acceptance band printed above each panel is $\tilde{q}^c \pm \tau_c$, where $\tilde{q}^c$ is the preliminary consensus and τ_c the median absolute deviation from it, so by construction roughly half of the supported teachers survive Stage 1.

Success case (Fig. 5c). On a ship image, five clients hold fewer than the peer median of 33 validation samples of the class and are dropped as uninformed before any weighting occurs. Of the remaining five, two fall outside the acceptance band and are discarded as consensus outliers. Of the three survivors, the client holding 166 ship samples receives 65.5% of the total weight and assigns 89.1% to the correct class, while the two lower-support survivors split the remainder. The aggregated target is therefore dominated by the one teacher that is both well-evidenced and confident, and it rises to 86.8% on the true class, well above the preliminary consensus of 68.7% that a uniform average would have produced.

Failure case (Fig. 5d). The same mechanism can suppress the teacher it should trust. On a dog image the peer consensus is low (31.4%), with a median deviation of $\tau_c = 11.8\%$. Client 7 holds 258 validation samples of the class, by a wide margin the best-evidenced teacher, and assigns 63.7% to the correct class. It is also the most accurate teacher on that class, at 90.5% in panel (b), so the filter is discarding the one teacher the weighting was designed to favor. Because that estimate lies 32.3 points from a consensus formed by less informed peers, Stage 1 removes it before Stage 2 can weight it. The surviving teachers all sit near or below the low consensus value, and the aggregated target ends at 24.6%, below even the consensus it started at.

This is the cost of consensus filtering under the assumption stated in Sec. 3.3, that unreliable teachers are in the minority for a class. Where that assumption holds the filter is protective, and where a well-supported specialist disagrees with a less informed majority it can remove useful signal. Letting support temper the consensus filter, rather than applying the two steps in sequence, is a natural refinement that we leave to future work.

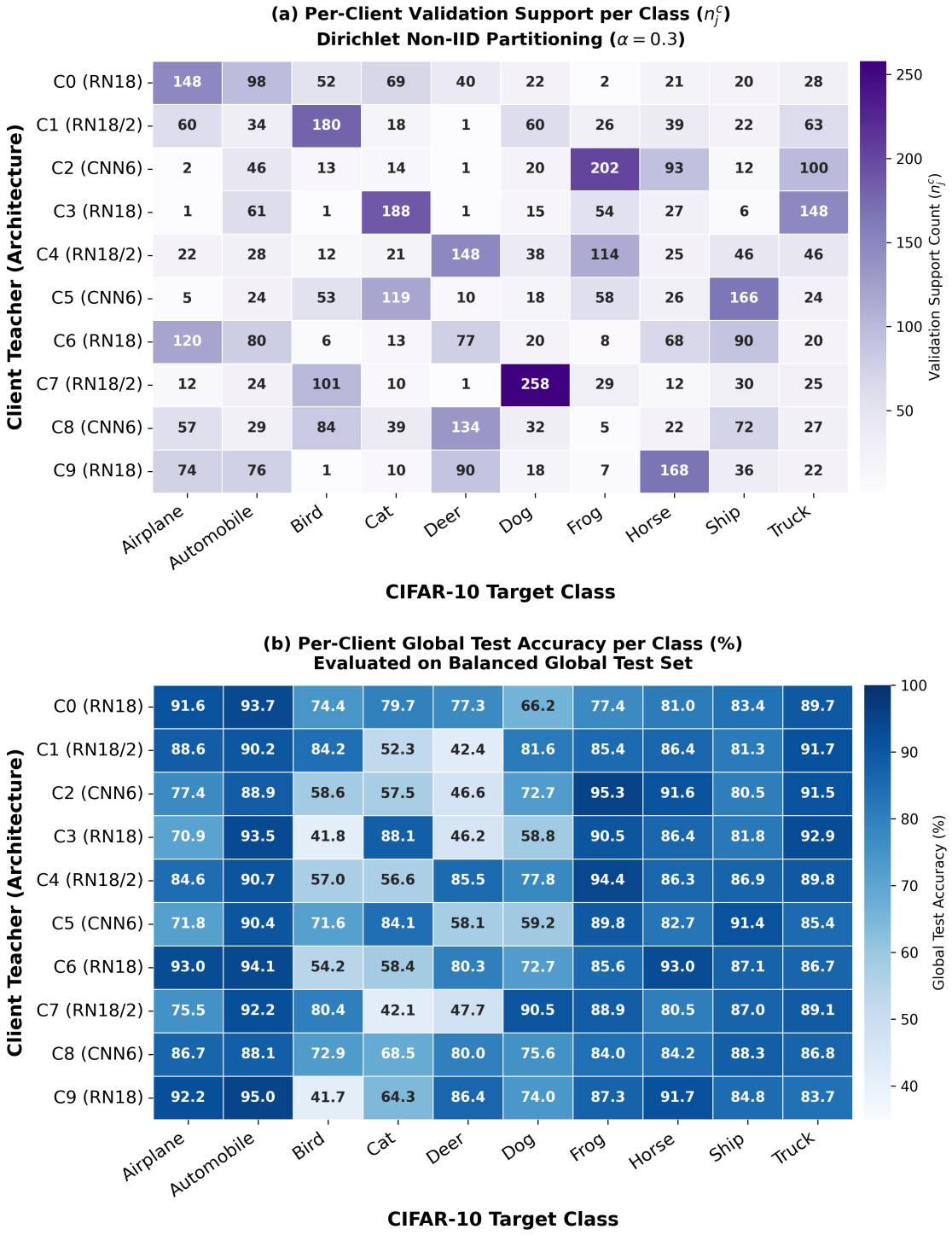


Figure 4. Context that drives the weighting, on CIFAR-10. **(a)** Per-client validation support n_j^c under the Dirichlet (α=0.3) partition, the count that enters the variance of Eq. 6 through Agresti–Coull smoothing. **(b)** Per-client accuracy on the balanced global test set, by class. The two are related but not identical, which is the reason CRAD weights on both accuracy and the evidence behind it rather than on either alone.



Figure 5. CRAD's two-stage aggregation traced on two individual CIFAR-10 test images. W is the assigned distillation weight after per-class normalization, the parenthesized value is the client's probability on the true class, and dev $= |q_j^c - \tilde{q}^c|$ denotes the client's absolute deviation from the preliminary consensus $\tilde{q}^c$. **(c) Success case, a ship image:** peers below the median support threshold ($n < 33.0$) are dropped as uninformed, two more fall outside the acceptance band $\tilde{q}^c \pm \tau_c$ and are dropped as consensus outliers, and the surviving well-supported specialist (C5, $n = 166$) receives 65.5% of the weight, raising the aggregated target on the true class to 86.8% from a preliminary consensus of 68.7%. **(d) Failure case, a dog image:** the best-evidenced teacher (C7, $n = 258$, and correct at 63.7%) deviates from a low consensus formed by less informed peers and is removed by Stage 1 (agreement filter), so its knowledge never reaches Stage 2 (precision weighting) and the target stays at 24.6%.